Local Density Fluctuation Governs the Divergence of Viscosity Underlying Elastic and Hydrodynamic Anomalies in a 2D Glass-Forming Liquid

Hayato Shiba,[1] Takeshi Kawasaki,[2] and Kang Kim[3]
[1]*Institute for Materials Research, Tohoku University, Sendai 980-8577, Japan*
[2]*Department of Physics, Nagoya University, Nagoya 464-8602, Japan*
[3]*Division of Chemical Engineering, Graduate School of Engineering Science, Osaka University, Osaka 560-8531, Japan*

(Received 14 May 2019; published 23 December 2019)

If a liquid is cooled rapidly to form a glass, its structural relaxation becomes retarded, producing a drastic increase in viscosity. In two dimensions, strong long-wavelength fluctuations persist, even at low temperature, making it difficult to evaluate the microscopic structural relaxation time. This Letter shows that, in a 2D glass-forming liquid, relative displacement between neighbor particles yields a relaxation time that grows in proportion to the viscosity. In addition to thermal elastic vibrations, hydrodynamic fluctuations are found to affect the long-wavelength dynamics, yielding a logarithmically diverging diffusivity in the long-time limit.

DOI: 10.1103/PhysRevLett.123.265501

In many two-dimensional ordering phenomena, fluctuations at long wavelengths are so strong that perfect order is destroyed. For example, the transition between a liquid and a crystalline solid is continuous or nearly continuous [1–6]. Recently, large-scale molecular dynamics (MD) simulations [7,8] and colloidal experiments [9,10] have revealed that such long-wavelength fluctuations also exist in two-dimensional (2D) liquids that are rapidly cooled toward the glass transition. Although retaining a random amorphous structure, elastic vibrations appear as the rigidity emerges with the decrease in temperature. The excess of low-frequency phonons in two dimensions [7,11] leads to an elastic anomaly, where the amplitude of thermal vibrations diverge at long wavelengths. Even in the presence of these long-wavelength fluctuations, the microscopic structural relaxations in 2D and 3D supercooled liquids appear to be similar, once the effect of these fluctuations has been eliminated by introducing quantities that characterize the local switching between neighbor particles [7,9,10].

Albeit a similarity of structural relaxation modality between 2D and 3D glass-forming liquids, it does not mean that the transport properties, a key to the nature of glass transitions, are similar in between. One problem lies in the relationship between the structural relaxation time and the viscosity. The glass transition is marked by a drastic increase in macroscopic viscosity with decreasing temperature, which is intimately related to the divergence of the microscopic structural relaxation time. As such, theoretical and computational studies have focused on the dynamical mechanism of growth in the microscopic structural relaxation time, most typically the α-relaxation time τ_α [12–15], defined as the decay time of the relaxation function for density fluctuations, i.e., the intermediate scattering function. However, in two dimensions, the strong density fluctuation diverges at long wavelengths and suppresses its intermediate plateau. Thus, τ_α no longer represents the microscopic structural relaxation time. The first problem arises on how to define the relaxation time that represents viscous slowdown of the dynamics.

Furthermore, a more intriguing problem lies in the potential role of hydrodynamic effects on the transport properties. For a liquid in two dimensions, a slow t^{-1} decay (the so-called long-time tail) of the velocity and stress autocorrelation functions leads to a *hydrodynamic anomaly* that is marked by a logarithmic divergence of transport coefficients such as diffusivity and viscosity [16–19]. How it alters the transport properties of deeply cooled liquids at the macroscopic level is a fully open issue, and the glass transition may be influenced by a mechanism that is different from the freezing of microscopic structural relaxation due to the cage effect. In fact, it is difficult to distinguish the characteristic timescales of the long-time tail and the microscopic structural relaxation, both of which become significantly large upon supercooling. Such long-wavelength fluctuations derived from hydrodynamics may even possibly prohibit the 2D glass transition. Therefore, in addition to the effect of elastic fluctuations that inhibit the existence of 2D crystals, it is important to reveal how macroscopic hydrodynamic fluctuations can influence the microscopic structural relaxation in 2D glass-forming liquids.

In this Letter, in order to address these issues, we perform large-scale MD simulations of a 2D glass-forming liquid and examine how the growth of various relaxation times is related to the divergence of macroscopic viscosity in the presence of long-wavelength fluctuations.

The simulations are performed with a particular focus on how the dynamics depend on the system size, so that the anomalous enhancement of elastic and hydrodynamic responses can be characterized. Simulations are performed for a 2D variant of Kob-Andersen binary Lennard-Jones mixtures [20], in which the composition is 65:35 [8,21–23]. The mixture is annealed for a sufficiently long time (maximum of 4×10^9 simulation steps) after rapid cooling to target temperatures in the range $0.4 \leq T \leq 1.0$ in the presence of Langevin heat baths. The production runs are then performed as Newtonian (NVE) dynamics simulations to prevent the damping of long-wavelength fluctuations. The data presented in the remainder of this Letter are averaged over four or eight independent simulations (Supplemental Material [24]).

First, we revisit three relaxation functions that have been considered in recent studies [7–10,23]. The first is the standard self-intermediate scattering function (SISF) $F_s(k,t) = (1/N)\langle\sum_{j=1}^{N}\exp\{i\boldsymbol{k}\cdot[\boldsymbol{r}_j(t+t_0)-\boldsymbol{r}_j(t_0)]\}\rangle$, with the wave vector set to $|\boldsymbol{k}| = 2\pi/\sigma_{11}$ so that its decay represents particle movement over a distance of the particle diameter σ_{11}. However, in two dimensions, long-wavelength elastic vibrations persist and these enhance the mean-squared thermal displacement δ^2 [7,25]. Figure 1 shows the SISF for a fixed temperature $T = 0.4$, where the size-dependent behavior is in agreement with previous studies [7,8]. The plateau heights represent the Debye-Waller factor $f_p \sim \exp(-k^2\delta^2/2)$ [24,26] and tend toward zero as the system size increases. Therefore, the α-relaxation time (the decay time of the SISF) is strongly influenced by long-wavelength fluctuations and cannot represent the microscopic structural relaxation time.

The other two functions are the "neighbor-relative" SISF (also known as the "cage-relative" SISF [9,10,23,27,28]) and bond relaxation function [22,29–31]. These are also plotted in Fig. 1. These functions characterize local structural relaxations. The former is defined by

$$F_s^R(k,t) = (1/N)\langle\sum_{j=1}^{N}\exp\{i\boldsymbol{k}\cdot\Delta\boldsymbol{r}_j^{\mathrm{rel}}(t)\}\rangle. \tag{1}$$

We here introduce the neighbor-relative displacement $\Delta\boldsymbol{r}_i^{\mathrm{rel}}(t) = (1/N_{\mathrm{n.n.}})\sum_{j\in\mathrm{n.n.}}[\Delta\boldsymbol{r}_i(t) - \Delta\boldsymbol{r}_j(t)]$ (also known as the cage-relative displacement [9,10,32]), where the summation is over $N_{\mathrm{n.n.}}$ initially neighboring pairs of particles, indicating the changes in the relative positions. A similar displacement was considered in previous studies on 2D crystalline melting for the same purpose of eliminating long-wavelength fluctuations [3,33,34]. The bond relaxation function $F_B(t)$, in contrast, does not involve displacements of the particles, but simply characterizes the proportion of initially neighboring pairs that have survived after a certain time (Supplemental Material [24]). From the observation that neither function is strongly dependent on the system size, contrary to the standard SISF, the effect of long-wavelength fluctuations is marginal for these relaxation functions, as expected from their definitions.

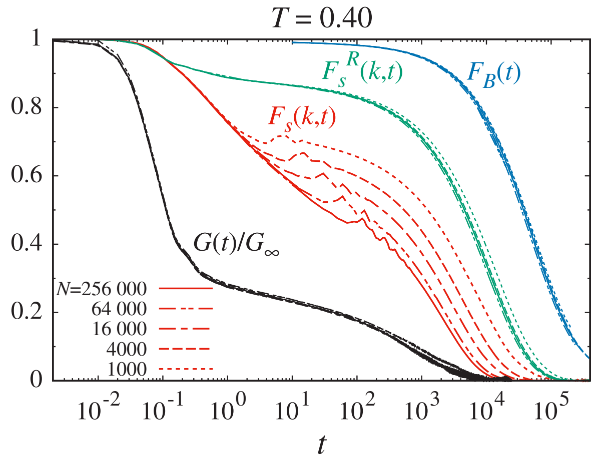

FIG. 1. Relaxation functions $F_s(k,t)$, $F_s^R(k,t)$, and $F_B(t)$ are plotted for system sizes $N = 256\,000$, 64 000, 16 000, 4000, and 1000 at $T = 0.40$. The corresponding stress relaxation function $G(t)$ is also plotted (normalized with respect to the instantaneous shear modulus G_∞).

Along with our aim to relate these microscopic relaxation functions with the macroscopic viscosity, Fig. 1 also shows the stress relaxation function (or "dynamic modulus" [23])

$$G(t) = \frac{V}{k_B T}\langle\sigma_{xy}(t)\sigma_{xy}(0)\rangle, \tag{2}$$

where $\sigma_{xy}(t)$ is the off-diagonal stress tensor [the data are normalized with respect to the instantaneous shear modulus $G_\infty = G(0)$]. $G(t)$ exhibits a stretched plateau modulus and no system-size dependence at a low temperature of $T = 0.4$, as shown in Fig. 1. In a recent study, the plateau was found to become unclear, rendering it difficult to evaluate the plateau modulus, for higher temperatures at the onset of slow dynamics, $T \geq 0.7$ [23].

Next, we define relaxation times and compare them with the transport coefficients—the α-relaxation time τ_α, neighbor-relative relaxation time τ_R, and bond relaxation time τ_B can be defined as the decay times of the standard SISF, neighbor-relative SISF, and bond relaxation functions (Supplemental Material [24]). For this purpose, we refer to the Stokes-Einstein (SE) relation $D\eta/T = \mathrm{const}$ between the diffusivity D and the viscosity η. This relation holds in normal liquids at high temperatures, but is violated in the deeply supercooled regime [21,31,35–37]. In simulation studies of glass-forming liquids, because the microscopic structural relaxation time is expected to grow proportionally with the viscosity, the left-hand quantity $D\eta/T$ (the so-called SE ratio) is often replaced by the product of the diffusivity and the relaxation time $D\tau_\alpha$, and its T dependence is usually examined. This assumption may break down in two dimensions because τ_α is robustly suppressed by the long-wavelength fluctuations. Thus, we calculate the temperature dependence of the generalized SE ratio $D\tau\,(\tau = \tau_\alpha, \tau_R, \tau_B)$ to examine how the three relaxation times change with respect to the diffusivity D as the temperature decreases. We further compare $D\tau$ with the original SE ratio $D\eta/T$. This is done by explicitly calculating the shear viscosity η via the Green-Kubo formula $\eta = \int_0^\infty G(t)dt$ [21,23], for which we require an error estimate because of the slow convergence of this integral (Supplemental Material [24]).

In Figs. 2(a)–2(c), the original SE ratio $D\eta/T$ is shown for system sizes of $N = 1000$, 16 000, and 256 000 as functions of the inverse temperature; the generalized SE ratios are also shown. Although the diffusivity D has a logarithmic dependence on the system size N, the generalized SE ratios can be meaningfully compared across different values of N because of their similar temperature dependence [24]. First, the standard SE ratio increases as the temperature decreases, as in 3D systems. However, $D\tau_\alpha$ exhibits system-size dependence and nonmonotonic temperature dependence and is clearly decorrelated from $D\eta/T$, which is consistent with the results of a previous study [21]. In contrast, $D\tau_R$ collapses to the standard SE ratio for all system sizes, showing that the neighbor-relative relaxation time τ_R grows in proportion to the viscosity, satisfying $\tau_R \sim \eta/T$ [see also Fig. 2(d)]. This relation provides an alternative to $\tau_\alpha \sim \eta/T$ [35,37–39], and thus τ_R clearly takes the role of the microscopic structural relaxation time. We also find that the generalized SE ratio for bond relaxation is preserved, i.e., $D \propto \tau_B^{-1}$, indicating that the bond relaxation function is a descriptor for the 2D diffusive motion in a similar manner to other 3D supercooled liquids [31,39].

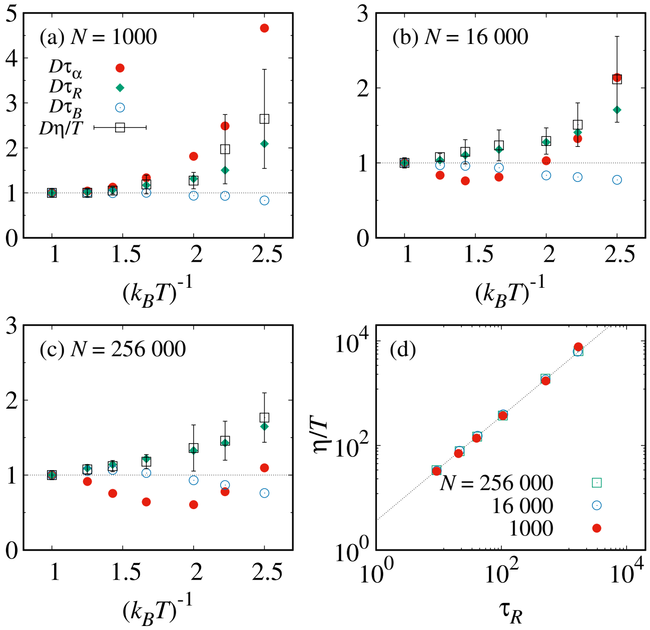

FIG. 2. (a)–(c) SE ratios for (a) $N = 1000$, (b) 16 000, and (c) 256 000 are shown as functions of the inverse temperature. Error bars indicate the standard deviation arising from the variation in η between independent runs. (d) η/T is plotted as a function of the neighbor-relative relaxation time τ_R for different N.

Thus far, we have seen that the diffusivity and viscosity are linked to timescales associated with local particle motion that is irrelevant to the long-wavelength fluctuations. However, this is not the end of our discussion, and we further investigate the hydrodynamic effects on the diffusivity by thoroughly examining the dependence on the system size. As shown in Fig. 3(a) for $T = 0.4$, the mean-squared displacements (MSDs) $\langle|\Delta\boldsymbol{r}(t)|^2\rangle = (1/N)\langle\sum_{i=1}^{N}|\boldsymbol{r}_i(t+t_0) - \boldsymbol{r}_i(t_0)|^2\rangle$ exhibit linear growth and remain dependent on the system size in the long-time limit. For temperatures $0.4 \leq T \leq 1.0$, we further estimate the diffusivity D by fitting $D = \langle|\Delta\boldsymbol{r}(t)|^2\rangle/4t$ in the long-time region $10 \leq \langle|\Delta\boldsymbol{r}(t)|^2\rangle \leq 20$ for different system sizes. The result is shown as a function of the box length L in Fig. 3(b). The diffusivity D grows logarithmically with system size, even at low temperatures. This size dependence cannot arise from a simple superposition of elastic vibrational fluctuations (the so-called Mermin-Wagner fluctuations [9]), but should be attributed to a different origin.

As a statistical measure for the motion of individual particles, the velocity autocorrelation function (VACF) $Z(t) = (1/d)\langle\boldsymbol{v}(t)\cdot\boldsymbol{v}(0)\rangle$ [19] contains information regarding the delay in the viscoelastic responses of liquids. Importantly, VACF is related to the diffusivity via the Green-Kubo formula $D = \int_0^\infty Z(t)\,dt$ and should provide clues as to the system-size dependence. However, calculating the full resolution of VACF for a glass-forming liquid

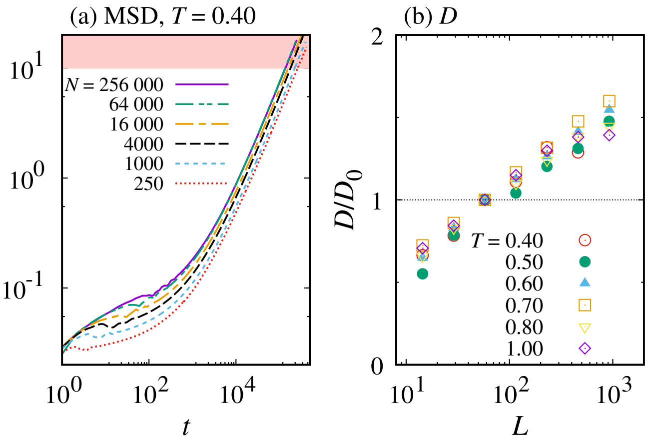

FIG. 3. (a) MSDs are plotted for system sizes $N = 256\,000$, 64 000, 16 000, 4000, 1000, and 250 at $T = 0.40$. The shaded region indicates the fitting region for evaluation of diffusivity. (b) Diffusivity D as a function of box length L. The corresponding particle number ranges over $250 \leq N \leq 1.024 \times 10^6$. For each temperature, the data are normalized with respect to D_0, the diffusivity at $N = 4000$.

is a difficult task, because random motions of the caged particles blur the slow process of diffusion. In a high-density 3D liquid at a moderately high temperature, the VACF exhibits a negative correlation in the intermediate time regions [40–42], which can be attributed to the velocity reversal caused by elastic vibrations of tagged particles [41]. Hence, for the present dense 2D liquid, we focus on high temperatures to demonstrate the crossover from transient elastic response to long-time hydrodynamic decay over a full time range. Figure 4(a) shows the VACF for different system sizes N at $T = 1.0$. Negative correlations exist for all N, indicating backward motion originating from elastic vibrations (see the plot for $N = 256\,000$ in the inset). However, the VACF does not simply decay from negative values to zero, but becomes positive over a longer time range for sufficiently large system sizes, such as $N \geq 256\,000$. By examining a much larger system size ($N = 4.096 \times 10^6$), the long-time limiting behavior is found to be consistent with the hydrodynamic t^{-1} tail that appears in normal 2D liquids [16–19,43,44]. Because the kinematic viscosity is large, i.e., $\nu = \eta/(nm) \gg D$, the analytical expression can be simplified to $Z(t) = (k_B T/8\pi\eta)t^{-1}$. Both the magnitude and power-law exponent of VACF coincide with this expression. Therefore, the system-size dependence of diffusivity D is attributed to the purely hydrodynamic origin in the long-time limit where the transient elastic response vanishes.

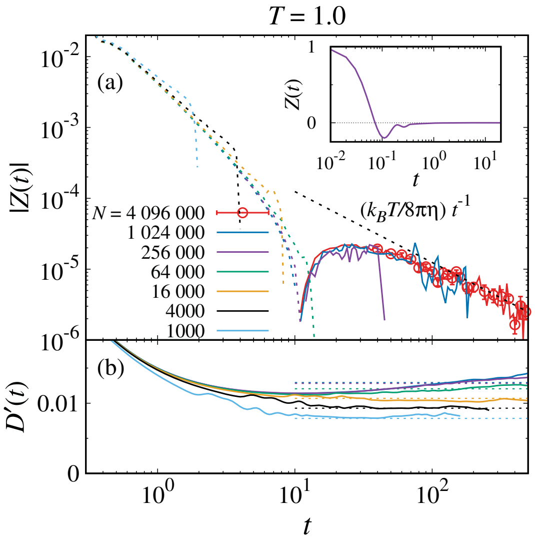

FIG. 4. (a) Absolute value of VACF $|Z(t)|$ for different system sizes at $T = 1.0$. The solid and dotted lines indicate that the corresponding VACFs assume positive and negative values, respectively. The data are only displayed over short time periods for small N, for ease of visibility. The straight line indicates the hydrodynamic long-time tail $Z(t) = (k_B T/8\pi\eta)t^{-1}$. (Inset) Semi-log plot of the raw value of VACF for $N = 256\,000$. (b) Time-dependent diffusivity, calculated by the Green-Kubo formula $D'(t) = \int_0^t Z(t)\,dt$ for different system sizes. Dotted lines indicate the diffusivity D evaluated from the MSD in Fig. 3(b).

Notably, the VACF itself exhibits system-size dependence at times before the t^{-1} power-law tail. For each N, the VACF exhibits a systematic decrease before becoming uncorrelated. In Fig. 4(b), we show the size dependence of the finite-time diffusivity

$$D'(t) = \int_0^t Z(t)\,dt, \tag{3}$$

in which the long-time limit yields the long-time diffusivity $D = \lim_{t\to\infty} D'(t)$. This finite-time diffusivity $D'(t)$ is in good agreement with the diffusivity D evaluated from MSD in the long-time limit. At the same time, it exhibits size dependence in an *earlier* time range, before converging to the long-time diffusivity D. Therefore, quite reasonably, the VACF $Z(t)$ itself is affected by the hidden hydrodynamic long-time tail, which has been difficult to find in simulations of 2D glass-forming liquids [21,23,36,45].

The above results suggest that the origin of the logarithmic divergence of diffusivity is the t^{-1} long-time tail and that it should exist even at low temperature. The long-time tail $Z(t) = (k_B T/8\pi\eta)t^{-1}$ no longer involves the diffusivity D in its expression and is free from the self-consistency problem leading to a faster than t^{-1} decay [18]. Therefore, the diffusivity simply diverges as

$$D \sim \frac{k_B T}{8\pi\eta} \ln\left(\frac{L}{\sigma_{11}}\right). \tag{4}$$

Hydrodynamic theories also predict the t^{-1} tail in the shear stress autocorrelation function, which may cause logarithmic divergence of shear viscosity [16]. The shear stress autocorrelation function is calculated for the same temperature but still such a power-law tail is not clear with the system size $N = 4.096 \times 10^6$ (Supplemental Material [24]).

It is worth noting that the analytic expression (4) brings about an increase of SE ratio $D\eta/T \sim \ln L$ over the entire range of temperature. This ratio increases by an order of magnitude if the system length L increases by 5 orders of magnitude. While a common expectation seems to be that the effect of the long-time tail is marginal in 2D glass transitions [45], it is clear that the long-time tail also causes violation of the SE relation, indicating that it may influence the 2D glass transition.

Finally, we address the relevance of our results to recent studies. A recent simulation study on the same 2D Kob-Andersen liquid reported that the mean square of the neighbor-relative displacement (i.e., cage-relative MSD) asymptotically approaches the normal MSD in the long-time limit [23]. Together with our observation of the finite-size effects in the MSD, their result implies that the neighbor-relative displacement is also system-size dependent, finally approaching the linear behavior of the usual MSD and giving rise to the same diffusivity. However, the neighbor-relative relaxation time τ_R is short enough that it remains virtually unaffected by the long-wavelength fluctuations. Therefore, our present results fully justify the use of the equivalent cage-relative SISF in recent colloidal experiments [9,10].

We note that our results rely on the use of the NVE ensemble to conserve the total momentum. Both the thermal vibrations and the hydrodynamic fluctuations at long wavelengths are suppressed by using the Brownian dynamics [8] or specialized Monte Carlo algorithms [46]. It has long been assumed that glassy dynamics are unaffected by the choice of ensembles, as in 3D liquids [47], but this is not the case in two dimensions for quantities that are affected by long-wavelength elastic and hydrodynamic fluctuations, including the standard SISF and the MSD.

In conclusion, the dynamics of a 2D glass-forming liquid are covered by hydrodynamic power-law correlations that lead to the logarithmic divergence of diffusivity, in addition to the recently revealed long-wavelength elastic fluctuations arising from the emerging rigidity of the liquid. Both the elastic and hydrodynamic fluctuations persist at long wavelengths to produce a concerted effect on the transport properties. Moreover, it is found that the relaxation time defined from the relative displacement between neighbors (τ_R) grows in proportion to η/T as the temperature decreases, implying that local density fluctuations govern the drastic increase in viscosity. The combined elastic and hydrodynamic anomalies are expected to be relevant to both the existence of the 2D glass transition [46] and the dynamical features of 2D crystal melting, although further clarification is required in forthcoming studies.

We thank Hajime Tanaka, Kunimasa Miyazaki, and Patrick A. Bonnaud for fruitful discussions. This work was supported by JSPS KAKENHI Grants No. JP18K13513 (H. S.), No. JP19K03767 (T. K.), and No. JP18H01188 (K. K.). H. S. was also financially supported by Building of Consortia for the Development of Human Resources in Science and Technology, Ministry of Education, Culture, Sports, and Technology (MEXT), Japan. The numerical calculations were performed on the Cray XC50-LC at the Institute for Materials Research, Tohoku University, Japan, the NEC LX406Rh-2 at the Research Center of Computational Science, Okazaki Research Facilities, National Institutes of Natural Sciences, Japan, and the SGI ICE XA and HPE SGI 8600 at the Institute for Solid State Physics, University of Tokyo, Japan.

---

[1] B. I. Halperin and D. R. Nelson, Theory of Two-Dimensional Melting, Phys. Rev. Lett. **41**, 121 (1978).

[2] K. Zahn, R. Lenke, and G. Maret, Two-Stage Melting of Paramagnetic Colloidal Crystals in Two Dimensions, Phys. Rev. Lett. **82**, 2721 (1999).

[3] Y. Han, N. Y. Ha, A. M. Alsayed, and A. G. Yodh, Melting of two-dimensional tunable-diameter colloidal crystals, Phys. Rev. E **77**, 041406 (2008).

[4] H. Shiba, A. Onuki, and T. Araki, Structural and dynamical heterogeneities in two-dimensional melting, Europhys. Lett. **86**, 66004 (2009).

[5] S. C. Kapfer and W. Krauth, Two-Dimensional Melting: From Liquid-Hexatic Coexistence to Continuous Transitions, Phys. Rev. Lett. **114**, 035702 (2015).

[6] A. L. Thorneywork, J. L. Abbott, D. G. A. L. Aarts, and R. P. A. Dullens, Two-Dimensional Melting of Colloidal Hard Spheres, Phys. Rev. Lett. **118**, 158001 (2017).

[7] H. Shiba, Y. Yamada, T. Kawasaki, and K. Kim, Unveiling Dimensionality Dependence of Glassy Dynamics: 2D Infinite Fluctuation Eclipses Inherent Structural Relaxation, Phys. Rev. Lett. **117**, 245701 (2016).

[8] E. Flenner and G. Szamel, Fundamental differences between glassy dynamics in two and three dimensions, Nat. Commun. **6**, 7392 (2015).

[9] B. Illing, S. Fritschi, H. Kaiser, C. L. Klix, G. Maret, and P. Keim, Mermin-Wagner fluctuations in 2D amorphous solids, Proc. Natl. Acad. Sci. U.S.A. **114**, 1856 (2017).

[10] S. Vivek, C. P. Kelleher, P. M. Chaikin, and E. R. Weeks, Long-wavelength fluctuations and the glass transition in two dimensions and three dimensions, Proc. Natl. Acad. Sci. U.S.A. **114**, 1850 (2017).

[11] H. Mizuno, H. Shiba, and A. Ikeda, Continuum limit of the vibrational properties of amorphous solids, Proc. Natl. Acad. Sci. U.S.A. **114**, E9767 (2017).

[12] F. H. Stillinger, A topographic view of supercooled liquids and glass formation, Science **267**, 1935 (1995).

[13] M. D. Ediger, C. A. Angell, and S. R. Nagel, Supercooled liquids and glasses, J. Phys. Chem. **100**, 13200 (1996).

[14] M. M. Hurley and P. Harrowell, Non-Gaussian behavior and the dynamical complexity of particle motion in a dense two-dimensional liquid, J. Chem. Phys. **105**, 10521 (1996).

[15] W. Götze, *Complex Dynamics of Glass-Forming Liquids: A Mode-Coupling Theory* (Oxford University Press, Oxford, 2009).

[16] M. H. Ernst, E. H. Hauge, and J. M. J. van Leeuwen, Asymptotic Time Behavior of Correlation Functions, Phys. Rev. Lett. **25**, 1254 (1970).

[17] B. J. Alder and T. E. Wainwright, Decay of the velocity autocorrelation function, Phys. Rev. A **1**, 18 (1970).

[18] M. A. van der Hoef and D. Frenkel, Evidence for Faster-than-t^{-1} Decay of the Velocity Autocorrelation Function in a 2D Fluid, Phys. Rev. Lett. **66**, 1591 (1991).

[19] J. P. Hansen and I. R. McDonald, *Theory of Simple Liquids* (Academic Press, New York, 2006).

[20] W. Kob and H. C. Andersen, Testing made-coupling theory for a supercooled binary Lennard-Jones mixture: The van Hove correlation function, Phys. Rev. E **51**, 4626 (1995).

[21] S. Sengupta, S. Karmakar, C. Dasgupta, and S. Sastry, Breakdown of the Stokes-Einstein relation in two, three and four dimensions, J. Chem. Phys. **138**, 12A548 (2013).

[22] E. Flenner and G. Szamel, Dynamic heterogeneity in two-dimensional supercooled liquids: Comparison of bond-breaking and bond-orientational correlations, J. Stat. Mech. (2016) 074008.

[23] E. Flenner and G. Szamel, Viscoelastic shear stress relaxation in two-dimensional glass forming liquids, Proc. Natl. Acad. Sci. U.S.A. **116**, 2015 (2019).

[24] See Supplemental Material http://link.aps.org/supplemental/10.1103/PhysRevLett.123.265501 for the following details: simulation settings, interpretation of the plateau height of the SISF, definitions of the relaxation times, the stress relaxation function and evaluation procedure of viscosity, and temperature dependence of diffusivity.

[25] B. Zhang and X. Cheng, Long-wavelength fluctuations and static correlations in quasi-2d colloidal suspensions, Soft Matter **15**, 4087 (2019).

[26] G. Pastore, B. Bernu, J. P. Hansen, and Y. Hiwatari, Soft-sphere model for the glass transition in binary alloys. II. Relaxation of the incoherent density-density correlation functions, Phys. Rev. A **38**, 454 (1988).

[27] H. Tong and H. Tanaka, Revealing Hidden Structural Order Controlling Both Fast and Slow Glassy Dynamics in Supercooled Liquids, Phys. Rev. X **8**, 011041 (2018).

[28] Y.-W. Li, C. K. Mishra, Z.-Y. Sun, K. Zhao, T. G. Mason, R. Ganapathy, and M. Pica Ciamarra, Long-wavelength fluctuations and anomalous dynamics in 2-dimensional liquids, Proc. Natl. Acad. Sci. U.S.A. **116**, 22977 (2019).

[29] R. Yamamoto and A. Onuki, Dynamics of highly supercooled liquids: Heterogeneity, rheology, and diffusion, Phys. Rev. E **58**, 3515 (1998).

[30] H. Shiba, T. Kawasaki, and A. Onuki, Relationship between bond-breakage correlations and four-point correlations in heterogeneous glassy dynamics: Configuration changes and vibration modes, Phys. Rev. E **86**, 041504 (2012).

[31] T. Kawasaki and A. Onuki, Slow relaxations and stringlike jump motions in fragile glass-forming liquids: Breakdown of the Stokes-Einstein relation, Phys. Rev. E **87**, 012312 (2013).

[32] S. Mazoyer, F. Ebert, G. Maret, and P. Keim, Dynamics of particles and cages in an experimental 2D glass former, Europhys. Lett. **88**, 66004 (2009).

[33] V. M. Bedanov, G. V. Gadiyak, and Yu. E. Lozovik, On a modified Lindemann-like criterion for 2D melting, Phys. Lett. A **109**, 289 (1985).

[34] K. Zahn and G. Maret, Dynamic Criteria for Melting in Two Dimensions, Phys. Rev. Lett. **85**, 3656 (2000).

[35] G. Tarjus and D. Kivelson, Breakdown of the Stokes-Einstein relation in supercooled liquids, J. Chem. Phys. **103**, 3071 (1995).

[36] B. Liu, J. Goree, and O. S. Vaulina, Test of the Stokes-Einstein Relation in a Two-Dimensional Yukawa Liquid, Phys. Rev. Lett. **96**, 015005 (2006).

[37] Z. Shi, P. G. Debenedetti, and F. H. Stillinger, Relaxation processes in liquids: Variations on a theme by Stokes and Einstein, J. Chem. Phys. **138**, 12A526 (2013).

[38] R. Yamamoto and A. Onuki, Heterogeneous Diffusion in Highly Supercooled Liquids, Phys. Rev. Lett. **81**, 4915 (1998).

[39] T. Kawasaki and K. Kim, Identifying time scales for violation/preservation of Stokes-Einstein relation in supercooled water, Sci. Adv. **3**, e1700399 (2017).

[40] B. J. Alder, D. M. Gass, and T. E. Wainwright, Studies in molecular dynamics. viii. The transport coefficients for a hard-sphere fluid, J. Chem. Phys. **53**, 3813 (1970).

[41] S. R. Williams, G. Bryant, I. K. Snook, and W. van Megen, Velocity Autocorrelation Functions of Hard-Sphere Fluids: Long-Time Tails Upon Undercooling, Phys. Rev. Lett. **96**, 087801 (2006).

[42] H. L. Peng, H. R. Schober, and Th. Voigtmann, Velocity autocorrelation function in supercooled liquids: Long-time tails and anomalous shear-wave propagation, Phys. Rev. E **94**, 060601(R) (2016).

[43] M. Isobe, Long-time tail of the velocity autocorrelation function in a two-dimensional moderately dense hard-disk fluid, Phys. Rev. E **77**, 021201 (2008).

[44] B. Choi, K. H. Han, C. Kim, P. Talkner, A. Kidera, and E. K. Lee, Nature of self-diffusion in two-dimensional fluids, New J. Phys. **19**, 123038 (2017).

[45] D. N. Perera and P. Harrowell, Origin of the Difference in the Temperature Dependences of Diffusion and Structural Relaxation in a Supercooled Liquid, Phys. Rev. Lett. **81**, 120 (1998).

[46] L. Berthier, P. Charbonneau, A. Ninarello, M. Ozawa, and S. Yaida, Zero-temperature glass transition in two dimensions, Nat. Commun. **10**, 1508 (2019).

[47] T. Gleim, W. Kob, and K. Binder, How Does the Relaxation of a Supercooled Liquid Depend on Its Microscopic Dynamics?, Phys. Rev. Lett. **81**, 4404 (1998).